R05-88

Available online at www.sciencedirect.com

SCIENCE DIRECT®

International Journal of Food Microbiology 99 (2005) 157–171

INTERNATIONAL JOURNAL OF Food Microbiology

www.elsevier.com/locate/ijfoodmicro

The mathematical properties of the quasi-chemical model for microorganism growth–death kinetics in foods

E.W. Ross, I.A. Taub, C.J. Doona*, F.E. Feeherry, K. Kustin

US Army RDECOM, Natick Soldier Center, Combat Feeding Directorate, Combat Feeding Innovative Science Team, Kansas St., Natick, MA 01760-5018, USA

Received 16 March 2004; received in revised form 5 July 2004; accepted 26 July 2004

Abstract

Knowledge of the mathematical properties of the quasi-chemical model [Taub, Feeherry, Ross, Kustin, Doona, 2003. A quasi-chemical kinetics model for the growth and death of *Staphylococcus aureus* in intermediate moisture bread. J. Food Sci. 68 (8), 2530–2537], which is used to characterize and predict microbial growth–death kinetics in foods, is important for its applications in predictive microbiology. The model consists of a system of four ordinary differential equations (ODEs), which govern the temporal dependence of the bacterial life cycle (the lag, exponential growth, stationary, and death phases, respectively). The ODE system derives from a hypothetical four-step reaction scheme that postulates the activity of a critical intermediate as an antagonist to growth (perhaps through a *quorum sensing* biomechanism). The general behavior of the solutions to the ODEs is illustrated by several examples. In instances when explicit mathematical solutions to these ODEs are not obtainable, mathematical approximations are used to find solutions that are helpful in evaluating growth in the early stages and again near the end of the process. Useful solutions for the ODE system are also obtained in the case where the rate of antagonist formation is small. The examples and the approximate solutions provide guidance in the parameter estimation that must be done when fitting the model to data. The general behavior of the solutions is illustrated by examples, and the MATLAB programs with worked examples are included in the appendices for use by predictive microbiologists for data collected independently.
© 2004 Elsevier B.V. All rights reserved.

Keywords: Predictive food microbiology; Quasi-chemical model; Chemical kinetics; Differential equation system; *Staphylococcus aureus*; *Escherichia coli*; Hurdles; High pressure processing

1. Introduction

The quasi-chemical model for microbial growth–death kinetics (Taub et al., 2003) is a unique mathematical tool for predicting microbial kinetics in food substrates. The model was developed in

0168-1605/$ - see front matter © 2004 Elsevier B.V. All rights reserved.
doi:10.1016/j.ijfoodmicro.2004.07.019

concert with the study of the growth kinetics of a cocktail of *Staphylococcus aureus* strains in intermediate moisture (IM) military bread (Feeherry et al., 2003) with variations in water activity (a_w, as adjusted by desorptive and absorptive techniques), pH, and temperature (T). In the latter study, both the logistic equation and Gompertz equation successfully fit the growth kinetics data and generated accurate estimates for the lag time (λ), maximum growth rate (μ), and asymptotic maximum (called ratio of growth and denoted as R_g). Some limitations with this approach were encountered. Microbial population data collected after completion of the stationary phase showed a decline, characteristic of the death phase of the bacterial life cycle (McMeekin et al., 1993; Bailey and Ollis, 1986; Lynch and Poole, 1979). For some data profiles, distinguishing late stationary phase data from early death phase data was ambiguous, and the resulting estimated value of μ depended on which data was included in the kinetics growth curve.

Microbial kinetics models generally fit either growth or death kinetics (Legan et al., 2002; Baranyi and Roberts, 2000; McMeekin et al., 1997; Whiting, 1995). Some alternative models have been proposed to account for microbial growth–decline data, such as the three-step enzyme kinetics model (Whiting and Cygnarowicz-Provost, 1992). Other models combine expressions for growth and death into a single equation, such as the logistic model with a superimposed Fermi term (Peleg, 1996), the Jones and Walker model (Jones and Walker, 1993; Jones et al., 1994), the Churchill model (Membré et al., 1997), and a model combining two Baranyi-type equations for yeast fermentation in a model wine system (Del Nobile et al., 2003). The Baranyi equation is a non-autonomous differential equation (Baranyi et al., 1993; Baranyi and Roberts, 1994) that is used to model microbial growth kinetics in foods (Membré et al., 1999), and whose mathematics have been studied extensively (Baranyi and Roberts, 1995).

The quasi-chemical model combines the concepts of chemical kinetics and predictive modeling in foods. Applying chemical kinetics to the macroscopic behaviors of microbial populations requires a much-simplified view of the network of biochemical reactions occurring in the microorganism (Bray and White, 1966; Hinshelwood, 1953). Insight into these complex metabolic processes can be gained from models based on chemical reaction mechanisms, and this approach has been used effectively in understanding nonlinear chemical dynamics such as oscillating chemical reactions (Epstein and Pojman, 1998). The chemically triggered alternation between independently living cells and cooperative aggregates of the cellular slime mold *Dictyostelium discoideum* was successfully modeled by introducing the chemical kinetics concept of autocatalysis (Goldbeter, 1991). Additionally, a predator–prey life cycle that was successfully duplicated in a controlled experiment utilizing planktonic rotifers feeding on algae in a chemostat was also modeled by integrating a biochemically based set of ODEs (Fussman et al., 2000). The quasi-chemical model postulates an underlying reaction scheme that combines autocatalytic growth and negative feedback, presumably in the form of a hypothetical antagonistic metabolite, which hastens the death of the actively multiplying cells. The actual chemical identity of this antagonist and its biomolecular mechanism have not yet been confirmed. One possibility is that the production of low levels of a diffusible metabolite by the bacterial cells acts as an intercellular signalling molecule and inhibits growth in the cell density-dependent gene expression phenomenon commonly referred to as *quorum sensing* (Smith et al., 2004; England et al., 1999; Novick, 1999; Bassler, 1999). Another possible negative feedback mechanism would involve the accumulation of a waste product such as lactic acid (Vereecken et al., 2003). A mechanism involving nutrient depletion (Leroy and De Vuyst, 2004) is less likely for describing the growth of a pathogen such as *S. aureus* in the nutrient-rich environment of a food product (Van Impe et al., 1999; McMeekin et al., 1993; Lynch and Poole, 1979).

From the proposed hypothetical mechanism, one can establish a set of kinetics rate equations that form the basis for a system of ordinary differential equations (ODEs) that imbue the quasi-chemical model with mathematical attributes. These attributes of the quasi-chemical model were originally used (Taub et al., 2003) to fit growth–death kinetics data and death-only kinetics for *S. aureus* in bread as functions of a_w, pH, and temperature. Statistical analysis of the results from the quasi-chemical model produced mathematical relationships among the parameters that were used to delineate a growth/

no-growth boundary in the pH–a_w plane. An interesting comparison showed that the quasi-chemical model estimated values of μ for the growth–death and growth-only data different from the value estimated with the Gompertz function (for the growth-only data). More recently, the quasi-chemical model has been generalized (Feeherry et al., 2004) to characterize the growth–death kinetics for other pathogens (*Escherichia coli* and *Listeria monocytogenes*) in foods (IM turkey meat, ham, and cheese) under various experimental conditions (a_w, pH, temperature, and lactate concentration). Additionally, the quasi-chemical model was successfully tested to account for the inactivation kinetics of *E. coli* in model foods using the emerging non-thermal technology of high pressure processing (Feeherry et al., 2004). Presently, we explore the mathematical properties of the quasi-chemical kinetics model that make it a useful tool for predictive microbiology. We examine the mathematical relationships among the parameters that give the quasi-chemical model the ability to fit growth–death kinetics and (linear and nonlinear) death kinetics satisfactorily. In Appendix A, we list the MATLAB programs that can be used to fit data by this model, and Appendix B describes a worked example of a typical data set using these programs. The authors would be pleased to provide electronic versions of these programs upon request.

2. Material and methods

2.1. The quasi-chemical model

Table 1 briefly summarizes the theoretical basis of the quasi-chemical model; namely, the hypothetical four-step reaction scheme, and the corresponding rate equations and system of ODEs (Taub et al., 2003). The concentration of lag phase cells is denoted by M, growth phase cells by M^*, antagonist by A, and dead cells by D. The concentrations and rate constants (k_1 through k_4) have only non-negative values. The procedures for making initial estimates for these parameters and determining quantities such as maximum logarithmic growth rate (μ), lag time (λ), maximum population size (called the ratio of growth and denoted R_g) are described in subsequent sections.

Table 1
Summary of mechanism and equations for the quasi-chemical model

Reaction step	Rate equations	ODEs	
$M \rightarrow M^*$	$v_1=k_1M$	$dM/dt = (-v_1) = -k_1M$	(1)
$M^* \rightarrow 2M^*+A$	$v_2=k_2M^*$	$dM^*/dt = (v_1+v_2-v_3-v_4)$ $= k_1M + M^*(G-\varepsilon A)$	(2)
$M^*+A \rightarrow D$	$v_3=k_3M^*A$	$dA/dt = (v_2-v_3) = M^*(k_2-\varepsilon A)$	(3)
$M^* \rightarrow D$	$v_4=k_4M^*$	$dD/dt = (v_3-v_4) = M^*(k_4+\varepsilon A)$	(4)
		$U(t) = M(t) + M^*(t)$	(5)

The net natural growth rate, G ($G \equiv k_2-k_4$), depicts the excess of the growth rate over the natural death rate. The parameter e relates to k_3 by $e=hk_3$, in which the scaling factor h (defined as $h=\varepsilon/k_3$) is assigned the value 10^{-9} (and consequently $(0 \le \varepsilon \ll 1)$ to facilitate numerical solutions of the ODEs. The initial conditions at $t=0$ are as follows: M equals I (the inoculum level, $I \approx 10^3$–10^4), and $M^*=A=D=0$. Changes in the microbial population size are represented by the quantity $U=M+M^*$ (in units of CFU/mL) and are derived from microbiological plate counts that do not distinguish lag phase (M) and growth phase (M^*) cells (see Table 1, Eq. (5)). Fig. 1 (Taub et al., 2003) depicts the behavior of the individual entities in the quasi-chemical mechanism (M, M^*, A, D, and U) from the fit of a typical set of growth–death kinetics data.

3. Results

3.1. Properties of the model

The growth–death profile of $U(t)$ shown in Fig. 1 is based on a non-zero value of k_3 ($k_3=100$) and a positive value of G ($k_2-k_4=2$). When the relative values of the rate constants are varied, different patterns for U as a function of time are observed. Fig. 2 displays $U(t)$ with $G>0$ and fixed values of $k_1=1$, $k_2=4$, and $k_4=2$, while k_3 is varied incrementally from 0 to 1000. With values of $k_3>0$, the calculated function for U (and also for M^*—see Fig. 1) as a function of time depicts growth to a maximum followed by a decline. As k_3 becomes larger, the calculated $U(t)$ function becomes more pulse-like,

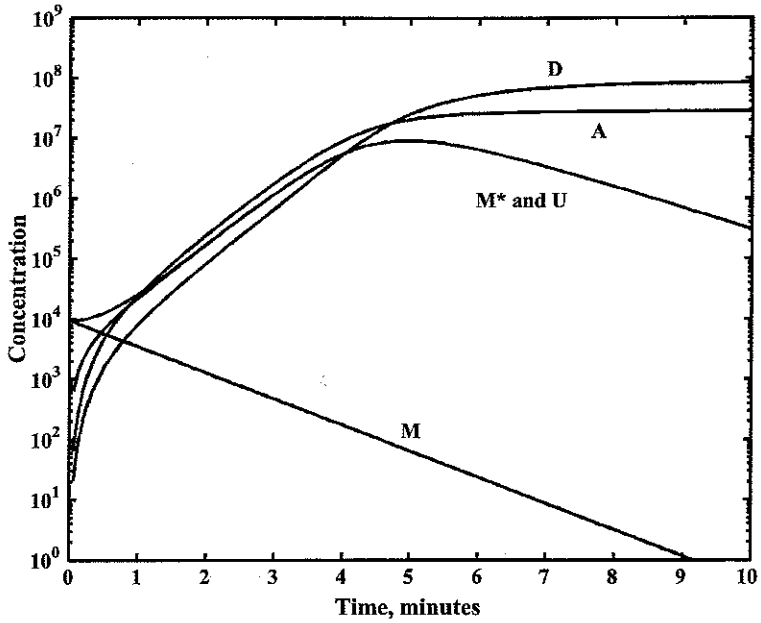

Fig. 1. Predicted plot of individual functions M, M^*, A, D, and U versus time with k_1=1, k_2=4, k_3=100, and k_4=2.

reaching its maximum earlier and at a lower value. When k_3=0, the function $U(t)$ shows limitless, nearly linear growth, which was not observed experimentally.

The ODE system (Table 1) is generally nonlinear due mainly to the interaction between the variables M^* and A in Eqs. (2) and (3), and solutions cannot

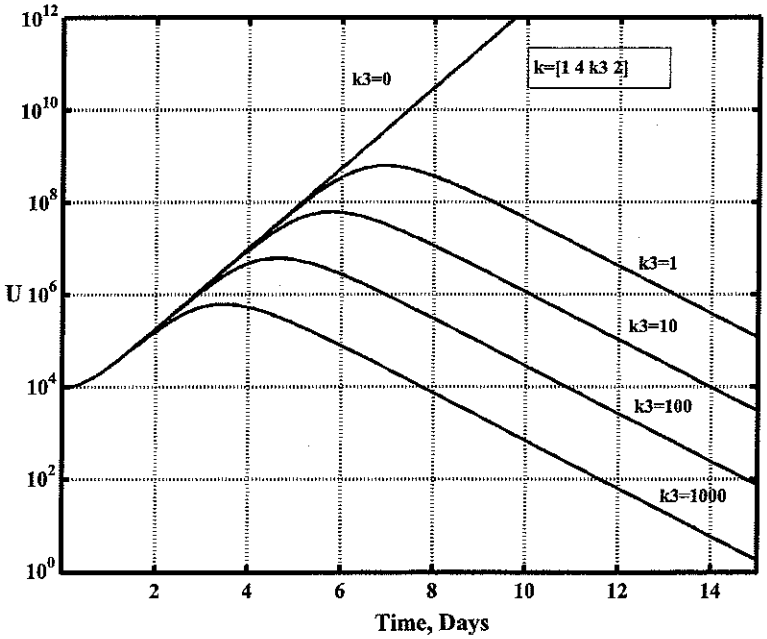

Fig. 2. Predicted effect of non-zero values of k_3 on growth–death behavior exhibited by $U(t)$ with {k_1=1; k_2=4; k_3=0, 1, 10, 100, 1000; and k_4=2}.

always be expressed by exact formulas. An exception is the solution to Eq. (1)

$$M = Ie^{-(k_1 t)} \tag{6}$$

that shows that M undergoes an exponential decline from I toward zero over time. The variable D is absent from Eqs. (1)–(3) and can be calculated from Eq. (4), after M^* and A have been determined (see Table 1). Since D does not influence the other variables, and M is known if k_1 is known, the relationship between M^* and A can be determined in the following way. First, assume that $M^*(t)$ is known, then solve Eq. (3) by elementary means (variation of parameters) according to Eq. (7)

$$A(t) = (k_2/\varepsilon)\left[1 - e^{-\phi(t)}\right]$$

$$\text{(in which } \phi(t) = \varepsilon \int_{s=0}^{s=t} M^*(s)\mathrm{d}s \geq 0) \tag{7}$$

Eq. (7) is not a solution for A, since M^* is not known, but rather an integral relationship between A and M^*. Differentiating Eq. (7) leads to $\mathrm{d}A/\mathrm{d}t = k_2 M^*(t)\mathrm{e}^{-\phi(t)} > 0$, which implies that $A(t)$ never decreases. Moreover, the quantity $[1-\mathrm{e}^{-\phi(t)}] \leq 1$, which when inserted into Eq. (7) leads to

$$A(t) \leq (k_2/\varepsilon) = k_2/(hk_3). \tag{8}$$

Consequently, $A(t)$ increases steadily from zero as time increases, but its value remains below the upper bound of k_2/hk_3 (see Fig. 1). The relationship between A and M^*, Eq. (7), establishes an essential feature of the ODE system (Table 1) when $k_3 \neq 0$. In the special case of $k_3=0$, this upper bound becomes irrelevant.

The interrelationship between A and M^* in response to variations in the values of the rate constants and their relative proportions can be seen in phase-plane plots. Figs. 3 and 4 show trajectories in the (M^*, A) phase plane using values of A and M^* obtained by numerical solution of Eqs. (1)–(4) and representative values assigned to the k's. The arrows in Figs. 3 and 4 indicate the direction of the respective trajectories as t increases from 0.1 to 10. In Fig. 3, the value of the rate constants are set {k_1=1; k_2=2, 3, 4, and 5; k_3=0; and k_4=4} such that k_3=0 and G ranges from negative to positive values. In these cases with k_3=0 and G>0, the model projects unrestrained growth of M^* and A. With k_3=0 and G<0, A increases

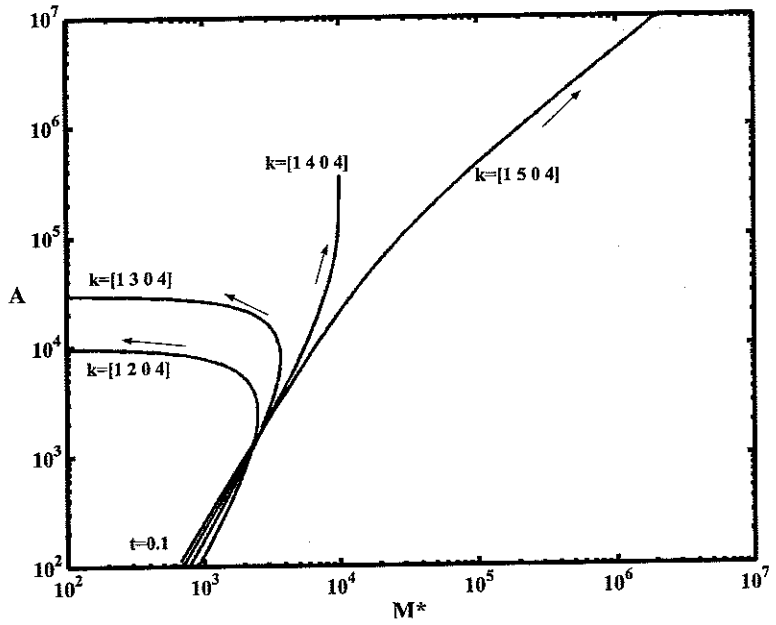

Fig. 3. Phase-plane plot [A, M^*] showing trajectories interrelating A and M^* with various values of G ($=k_2-k_4$) when k_3=0.

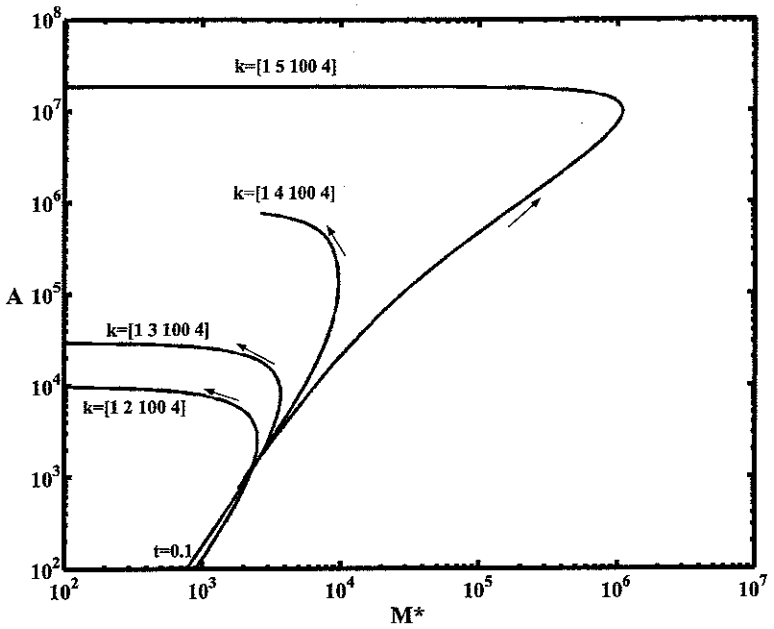

Fig. 4. Phase-plane plot [A, M^*] showing trajectories for various values of G when k_3=100.

toward a limiting value, and M^* changes only slightly, then decreases. Fig. 4 illustrates phase-plane plots with a set of rate constant values {k_1=1; k_2=2, 3, 4, and 5; k_3=100; and k_4=4} such that k_3>0 and G ranges from negative to positive values. With k_3=100 and G>0, the phase trajectories do not exhibit the limitless growth seen in Fig. 3. Instead, both M^* and A increase initially, then M^* eventually reaches a maximum and later declines, while A tends continuously toward a limiting maximum value. With k_3=100 and G<0, the trajectory behaves similarly to its k_3=0 and G<0 counterpart (Fig. 3). These results indicate that non-zero values of k_3 and positive values of G are needed to produce growth–death kinetics.

3.2. Behavior as $t \rightarrow \infty$

The critical points of the system (i.e. the points at which the system as a whole is stationary) must satisfy the following conditions

$$dM/dt = 0 = -k_1 M \tag{9}$$

$$dM^*/dt = 0 = k_1 M + M^*(G - \varepsilon A) \tag{10}$$

$$dA/dt = 0 = M^*(k_2 - \varepsilon A) \tag{11}$$

$$dD/dt = 0 = M^*(k_4 + \varepsilon A) \tag{12}$$

Eq. (9) is satisfied when M=0, Eqs. (11) and (12) are satisfied when M^*=0, and Eq. (10) is satisfied when M=M^*=0. The lone critical point in this system occurs with M=M^*=0 and is reached only in the limit as $t \rightarrow \infty$. The values of $D(t)$ and $A(t)$, as mentioned previously for Eqs. (3) and (4), increase steadily towards constant values as $t \rightarrow \infty$ (see Fig. 1, for which k_3>0 and G>0).

3.3. Behavior near t=0

Approximate solutions of the following form are useful near the beginning of the process (when $t \approx 0$) and can be found by a Taylor series expansion about t=0:

$$M \approx I\left\{1 - k_1 t + \frac{k_1^2 t^2}{2}\right\} \tag{13}$$

$$M^* \approx k_1 I\left\{t + \frac{(G - k_1)t^2}{2}\right\} \tag{14}$$

$$A \approx \frac{k_1 k_2 I t^2}{2} \tag{15}$$

$$D \approx \frac{k_1 k_4 / t^2}{2} \tag{16}$$

$$U \approx I\left\{1 + \frac{G k_1 t^2}{2}\right\} \tag{17}$$

Eq. (14) shows that M^* increases initially from 0 approximately linearly, while A and D increase more slowly and in a quadratic fashion according to the ratio

$$\frac{A}{D} \approx \frac{k_2}{k_4}$$

U increases if $G>0$, and decreases if $G<0$. In all cases at $t=0$, $dU/dt=0$, and the model predicts that $U(t)$ always exhibits a non-zero value for the initial lag, although its duration may be immeasurably small. None of these approximations is affected by k_3. At sufficiently early times, solutions with $k_3=0$ are therefore acceptable approximations to the true solutions.

3.4. Approximation when $k_3=0$

In examples with $k_3=0$, the nonlinear terms disappear from the ODE system, and the effect of A on the microbial kinetics is negligible. In this case, exact solutions for M^*, A, and U can be found by elementary means as follows:

$$M^* = k_1 I f(t,m) e^{Gt} \tag{18}$$

$$U = I\{e^{-mt} + k_1 f(t,m)\} e^{Gt} = I\{e^{-k}1^t + k_1 f(t,m) e^{Gt}\} \tag{19}$$

$$A = (I k_1 k_2 / m)\{f(t, -G) - f(t, k_1)\} \tag{20}$$

with the definitions

$$m = G + k_1 = k_1 + k_2 - k_4 \tag{21}$$

$$f(t,m) = (1 - e^{-mt})/m \tag{22}$$

A special case occurs when k_1 is very large. These conditions are uncommon and require special circumstances that will be discussed later. Specifically, when $k_1 \gg |G|$, the value of $m \approx k_1 \gg 1$, and accordingly $f(t,m) \approx 1/m$. After a brief time increment elapses, $M \ll M^*$ and $U \approx M^*$.

As described in the previous section, k_3 exerts little influence in the early stages, and the approximate solutions for $k_3=0$ (Eqs. (18)–(22)) can be used.

$$U \approx M^* \approx (k_1 I/m) e^{Gt} \text{ and } \ln(U) \approx \ln(k_1 I/m) + Gt$$

When $k_3=0$, Eqs. (2) and (3) lead to the equation

$$dU/dt = dM/dt + dM^*/dt = GM^*$$

$$= G k_1 I f(t,m) e^{Gt}$$

Thus, dU/dt has the same sign as G, which indicates that U always increases with t if $G>0$, and correspondingly U always decreases if $G<0$. Growth–decline kinetics (Taub et al., 2003) cannot be predicted by the formulas derived with $k_3=0$ in Eqs. (18)–(22). Relatively large values of k_3 are needed for the quasi-chemical model to depict the growth–death phenomenon characteristic of the microbial life cycle.

The relation of the maximum (logarithmic) growth rate (μ) and G is consistent with these findings. Let

$$L = L(t) = \log_{10}\{U(t)\}, \text{ then } L \approx \log_{10}(k_1 I/m) + BGt$$

in which $B=\log_{10}(e)=0.4343$, and the slope of L is approximately constant,

$$dL/dt \approx BG$$

$$\mu = \max\{dL/dt\} \tag{23}$$

Since dL/dt is approximately constant, this equation yields the relation

$$\mu \approx BG \tag{24}$$

Fig. 5 shows a plot of μ versus G using previously reported values obtained from modeling the growth–death kinetics of *S. aureus* in IM bread at various conditions of a_w, pH, and temperature (Taub et al., 2003). The straight-line graph of Eq. (24) shows that the latter is a good predictor of this relationship, except possibly when $|G|$ is near zero. This estimate is consistent with the conclusion that μ usually occurs early enough in the process to justify the application of the approximate solutions obtained for $k_3=0$.

3.5. The death-only case

The quasi-chemical model also fits death-only kinetics observed as a result of "no-growth" con-

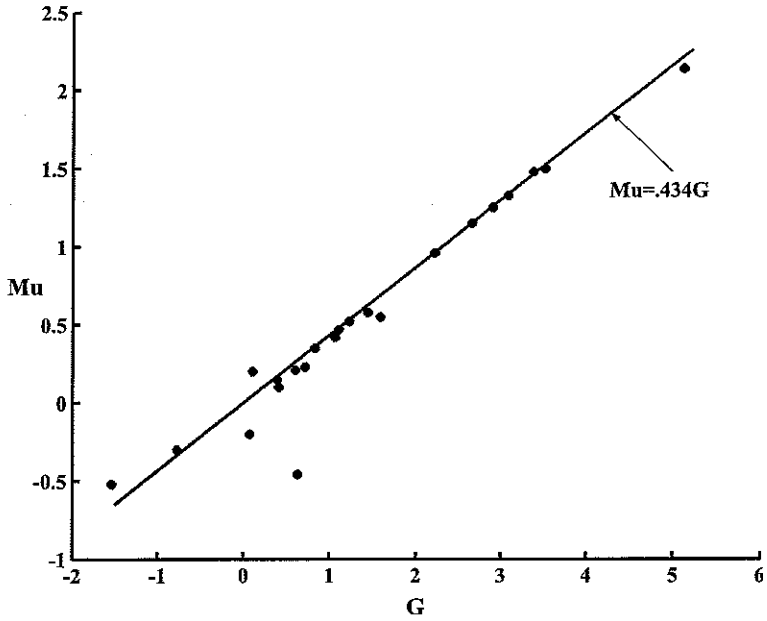

Fig. 5. Linear relationship of μ and G (values obtained from fitting with the quasi-chemical model) in accordance with Eq. (24) (μ=BG).

ditions of a_w, pH, and T (Taub et al., 2003), or from the application of high hydrostatic pressure (Feeherry et al., 2004). The fitting procedure in these cases leads to two entirely different sets of parameters (called the "fast set" and the "slow set") that fit the data equally well. For example, the fitted lines calculated by the "fast" and "slow" sets for the high pressure (P=50,000 psi) inactivation of *E. coli* in whey protein (Feeherry et al., 2004) are nearly identical, and the corresponding estimates of μ are also very similar ($\mu \approx -0.12$, see Table 2).

Both the "fast" and "slow" parameter sets have negligible values for k_3, and solutions are approximated using Eqs. (18)–(22). The "fast set" features large values of k_1 ($k_1 \gg 1$), and $M^* \gg M$ shortly after t=0, while the "slow set" has small values of k_1 and $M^* \ll M$. In cases with negligibly small lag times (especially those involving high pressures), the plot of $\log(U)$ versus t is approximately linear, and Eqs. (18)–(22) show that [$G_{(\text{fast set})} \approx -k_{1(\text{slow set})}$]. Although the functions U are nearly identical in both sets, the different parameters calculate very distinct temporal functions for M, M^*, A, and D (Figs. 6 and 7). The most notable differences are the rapid decay of M and rapid production of M^* in the fast set (Fig. 6), in comparison to the slow decay of M and the slow rise–fall kinetics of M^* generated by the slow set (Fig. 7). With the slow set, the production of A is also significantly delayed and the evolution of D is slightly attenuated.

Table 2
"Fast set" and "slow set " from fitting microbial inactivation data

	k_1	k_2	k_3	k_4	G	μ
"Fast"	34.30	0.96	0	10.25	−0.282	−0.12
"Slow"	0.282	0.70	0	19.31	−18.62	−0.12

3.6. Model fitting and parameter estimation

Nonlinear least-squares analysis was used to obtain best-fit values of the model parameters (rate constants k_1 through k_4) by solving numerically the ODE system for the four state variables M, M^*, A, and D which lead to the estimate of the measurement variable, $U(t)$. This procedure was carried out using MATLAB software, specifically the stiff differential equation solver ODE15s, in conjunction with the nonlinear regression analysis program

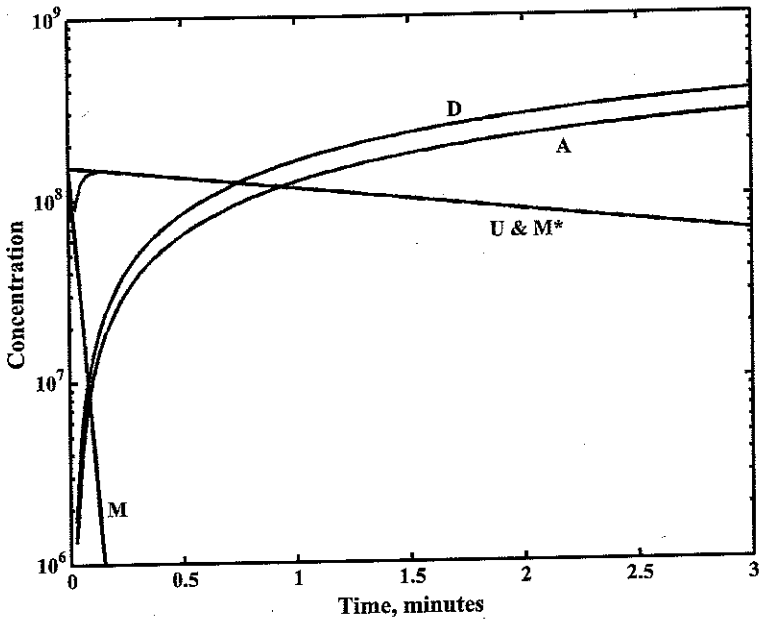

Fig. 6. Plots predicting M, M^*, A, D, and U versus time for death kinetics using "fast set" of parameters.

LSQNONLIN. These programs (see Appendices A and B) require initial estimates for the k's and iteratively seek the values of k's that generate the smallest sum of squared errors. Generally, the least-squares fitting procedure worked well for data that were not too noisy, but the goodness of fit depended on fortuitous initial estimates of the k's. Like many nonlinear searching programs, LSQNONLIN may fail

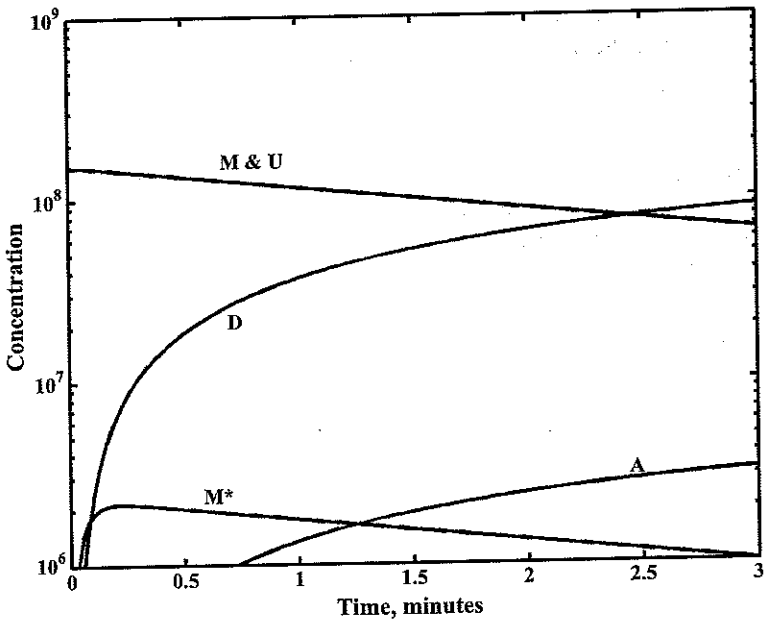

Fig. 7. Plots predicting M, M^*, A, D, and U versus time for death kinetics using "slow set" of parameters.

if the initial choices are bad. Also, the initial estimates can appear to influence the final results if the data are irregular or too sparse. While no general procedure will help in all cases, it is possible to state the following rules of thumb using the information about the mathematical properties of the model described above:

(A) If the data appear to start by growing, choose initial estimates having $k_2>k_4$, and choose $k_2<k_4$ if the data decline with time.
(B) Increasing k_1 generally speeds up the process.
(C) If there is enough data near the start of the process, Eqs. (13) and (17) may suggest an initial estimate of G.
(D) In program SD in Appendix A, the line that begins LB=[. . . allows the user to specify lower and upper bounds in the search for parameter values. For example, if we think that $k_1 \approx 2$, we can simplify the search by setting LB=[1.9 1 1 1]; UB=[2.1 1 1 1] on that line.

The value of μ was estimated by numerically differentiating $L(t)=\log_{10}(U(t))$ to find its slope and searching for the maximum of that slope. In cases where only death occurred, μ was determined from the minimum slope of $L(t)$ as a negative growth rate. If the time at which μ occurs is defined as t_μ, then the lag (denoted λ) is estimated from the formula

$$\lambda = t_\mu - \left(L_\mu - L_o\right)/\mu.$$

where

$$L_o = L(0) \text{ and } L_\mu = L\left(t_\mu\right)$$

The ratio of growth (R_g) characterizes the extent of multiplication of the initial organism concentration (asymptotic maximum). The quantity R_g is expressed by the relation

$$R_g = \log_{10}\{\max[U(t)]/U(0)\} \quad (25)$$

The quantity R_g applies only to situations involving growth, and R_g has the value of zero, in cases when only death kinetics are observed ("no-growth" conditions).

4. Discussion

The current models used most commonly for microorganism kinetics (Gompertz or logistic equations) tend to focus exclusively on either growth or inactivation, and generally ignore the death phase when it succeeds growth. The quasi-chemical model (Taub et al., 2003), like some reported alternatives, has the capacity to model continuously growth–death kinetics and incorporates death data in the estimation of the growth kinetics parameters. This feature is advantageous, when there is a paucity or irregularity in the growth data, and also eliminates the need for subjectivity when determining which stationary phase data constitute the endpoints of the growth curve.

The quasi-chemical model consists of four autonomous ODEs for four variables (M, M^*, A, and D) which together specify the system and the predicted microorganism concentration, $U(t)$. Even this rudimentary representation of the microbial life cycle provides some insight into the metabolic activities governing the closed-system behavior of the bacterial cell. Specifically, the model predicts (at least) two different pathways to death, one that occurs in no-growth conditions and another that prevails after a period of robust growth through a mechanism involving negative feedback. Bacteria are known to produce substances that inhibit growth, some in the form of diffusible molecules that act in a cell density-dependent way to influence specific gene expression, called *quorum sensing* (Smith et al., 2004; England et al., 1999; Novick, 1999; Bassler, 1999), and others in the form of organic acids (Vereecken et al., 2003). We do not present experimental evidence to confirm the presence, identity, or mechanism of the hypothetical antagonist in the quasi-chemical model that is proposed to act in a manner analogous to these known inhibitors. The present results do not contradict the hypothesis that there is more than one pathway to death of the organism, and that metabolic by-products influence the rate of the alternate pathways.

The quasi-chemical model is an ODE model based on the simple premise that the mathematical model comprises one or more differential equa-

tions. Presently, the ODE model contains four parameters (k_1 through k_4) that specify the model behavior and are estimated by fitting the data (U). The ODEs are generally nonlinear due to the interaction of M^* and A in the proposed mechanism, and this relationship is critical for reproducing growth–death kinetics. Solutions to the ODEs obtained through various approximations show that the behavior of U depends principally on certain values for the quantities k_3 and G. Specifically, only if $k_3>0$ and $G>0$, will $U(t)$ show growth–decline behavior. If $k_3\geq 0$ and $G<0$, then only death occurs. The value of μ is linearly related to G (see Eq. (24) or Fig. 7), but λ and R_g are not closely associated with G or the k's. The parameter k_1 affects primarily the overall time-scale of the process, and the relation between M^* and A is not directly affected by changing k_1 (Eq. (7)). The approximations made when $k_3=0$ are influenced by the quantity m, which depends on k_1 (Eq. (21)). If $k_3=0$, the model predicts that U grows without limit when $G>0$, and declines when $G<0$. None of the data exhibited unlimited growth.

The quasi-chemical model adequately characterizes the death-only case (when $G<0$) in the sense that it can satisfactorily fit the $U(t)$ data and estimate a value for μ. In its present form, the model lacks uniqueness, since at least two sets of parameters may provide equally good fits of the data. In fact, all sufficiently large values of k_1 in the "fast set" that induce M to become negligible quickly will also produce nearly identical values of $U(t)$. Eq. (19) justifies this statement; the relationship $m\approx k_1\gg 1$ implies $k_1 f(t,m)\approx 1$, and $U\approx Ie^{Gt}$ (i.e. U depends only on G and not k_1). For some purposes, this non-uniqueness is not detrimental. It suggests that the model in its current form may be over-parameterized for death-only kinetics, but also leaves open the question of which parameter set more closely resembles the true dynamics. Both parameter sets are equally valid in terms of mathematics, and more experimental data would be needed to distinguish which is more appropriate from a microbiological perspective. This uncertainty does not affect the determination of $U(t)$ or μ, although there is ambiguity in the definition of μ when $G<0$. The present definition leads to quantitative characterization of the death rate as $(-\mu)$, but other definitions are possible and could be a subject for future study. In cases where only growth kinetics data are collected, a cursory exploration of existing data suggested that in the fitting process the resulting estimates of the k's might sometimes depend on the initial estimates of these parameters. However, as in the death-only case, the changes in the k's did not appear to affect the estimates of U or μ significantly.

Acknowledgements

The authors wish to express their gratitude to Mr. James Doona (Mathematician), Dr. Jack Briggs (Senior Food Technologist), and Dr. Fred Allen (Chemical Engineer) for providing helpful discussions and insight into issues regarding mathematics, fermented food products and bioprocess engineering.

Appendix A. MATLAB programs for fitting the ODE model

These programs for fitting the data by the ODE model consist of a MATLAB script, SD, that invokes the nonlinear least-squares function LSQNONLIN which calls the function, ED, to assist in the fitting. ED uses MATLAB program ODE15S to solve the ODE system which is defined in the function FD. The separate MATLAB script PredODE simply calculates the solutions, M, M^*, A, D, and U, given the k values and the initial variable values; it does not involve any fitting of data but does solve the ODE system. Each of these programs must be stored in a file having the same name as the program, e.g. SD must be stored in a file named SD.m. The percent symbol, %, in the programs denotes that the remaining text on that line is merely commentary. In these programs, the variables M, M^*, A, and D are re-named in matrix fashion as follows:

$$M = x_1 = x(:,1);\ M^* = x_2 = x(:,2);\ A = x_3 = x(:,3);\ D = x_4 = x(:,4).$$

```
% Script SD.m

% This script calls nonlinear least-squares solver LSQNONLIN to find the
% values of p that minimize the differences between the ODE solution and
% the data. p contains the values of k that are varied during the fitting. Other
% members of k are held constant. Function ED  calculates the errors at data
% values. Before running this script,  the following quantities must be
% defined in the main program:
%   td is a row vector of times at which concentrations are measured.
%   xd is a row vector of concentrations  (not the log of concentrations)
%   k is a row vector of initial parameter estimates
global  x
Ld=log10(xd);
x0=[xd(1) 0 0 0 ];  % Initial values of the x's are defined here
p0=k;
LB=[0 0 0 0]; UB=[1000 10000 1000 1000];    % LB and UB define bounds on parameters
options=optimset('Display','iter');  % This causes display of intermediate results
[p,Nm,Errorvector]=lsqnonlin('ED',p0,LB,UB,options,x0,td,Ld); % Nonlinear Least Squares
                                                              % Optimizer
U=x(:,1) + x(:,2); Lx=log10(U);   % Lx is the model-prediction of  Log(U)
plot(td,Ld,'o',td,Lx); xlabel('Days'); ylabel('Log Cols'); grid;   % This plots  Ld and Lx vs t
SS=(Nm)^0.5       % Square root of sum of squared errors in the fit
k=p               % This causes the k's to be listed in the output
[td' Ld' Lx Errorvector]     % The time-history of Ld and Lx  is listed in  the output
% End of Script SD.m ----------------------------------------------------------------

   Function ED.m
% This function, ED.m, calculates the vector of mismatches between the
% data and the model predictions for given parameters, k. The model
% predictions are found by solving the ODE system, using solver ODE15S.
% ED is called by Script SD and calls function  FD to  specify the ODE
% system.
function Err=ED (p,x0,td,Ld)
global  x
k=p;
options=odeset('Abstol',1e-12,'Reltol',1e-4);
[t,x]=ode15s('FD',td,x0,options,k);    % Stiff ODE solver
U=x(:,1) + x(:,2);
Lx=log10(U);
Err=Ld'-Lx;      % Err is the vector of  errors in the prediction of the model
% End of function ED.m ---------------------------------------------------

Function FD.m
% This function, FD.m, defines the ODE system to be solved for given
% parameters, k, in finding the model predictions. It is called by function ED.
function dx=FD (t,x,flag,k)
% Rate Functions:
    h = 1e-9;
   v1=k(1)*x(1);              v2=k(2)*x(2);
   v3=h*k(3)*x(2).*x(3);   v4=k(4)*x(2);
% ODE definitions in terms of rates:
dx=zeros(4,1);
dx(1)=-v1 ;              % x(1) = Concentration of Organisms in Lag Phase
dx(2)=v1+v2-v3-v4;  % x(2) = Concentration in Growth Phase
dx(3)=v2-v3;             % x(3) = Concentration of Antagonist
dx(4)=v3+v4;             % x(4) = Concentration of dead Organisms
% End of Function FD.m  ------------------------------------------------
```

```
% Script PredOde.m
% This script, PredODE.m, uses the ode-solver to predict the solutions,
% x1 to x4, for given k-values. It calls the function "FD" to specify the ODE
% system, prints a graph of Log(U) vs t and calculates μ, λ and Rg. Before
% running this script you must define the values of k in the main program.
x0=[1e4 0 0 0];                % This defines the initial values of the x's.
mesh=.2; tr=[0:mesh:20]';      % This defines the times at which the x's are evaluated.
options=odeset('Abstol',1e-12,'Reltol',1e-5);
[t,x]=ode15s('FD',tr,x0,options,k);   %Stiff ODE solver
U=x(:,1) + x(:,2) ; Lx=log10(U);
semilogy(t,U); xlabel('Days');ylabel('Col Count');grid; % This causes plotting of U(t)
DL=diff(Lx);
Lslp=DL/mesh;
[MuL,IL]=max(Lslp)             % MuL is the estimate of μ
tmL=tr(IL);                    % IL is the index of the time of maximum slope
Lo=Lx(1);
Lmu=Lx(IL);
Lambda=tmL+(Lo-Lmu)/MuL  % Lambda is the estimate of λ
RA=Lx-Lo;
Rg=max(RA)                     % Rg is estimated here
[R C]=size(tr);
if k(2)-k(4)<0
  Muneg=Lslp(R)          % Muneg is the estimate of μ when only death occurs.
  end
% End of Function PredODE.m
```

Appendix B. Output of comparison calculations

Below we show the input and output for a MATLAB fitting of a typical data set. First, we display the results for the ODE model. The solicitation symbol, ≫, displayed by MATLAB, indicates that we are expected to enter something from the keyboard. The first three entries are the input, which defines the quantities td, xd, the time and concentration, i.e. the test data that we are trying to fit, and k, our initial guesses for the parameters. Next is the command, SD, to execute the script SD. This is followed by output from SD. The first block of output gives information about the intermediate steps in the repetitive process that LSQNONLIN uses. Generally, $f(x)$ and the Norm of Step should both decrease, but the latter may occasionally increase slightly from one iteration to the next. We do not list below all the steps in the iteration, but only the first few and last few. The output may depend slightly on the computer and operating system on which this is run.

```
>> td =[0  1  2  3  4  5  6  7  8  9  10  11  12  14];

>> xd =[7680 24000 1.07e6 1.98e7 9.58e7 2.06e8 1.08e8 1.66e8 ...
     5.39e7 1.07e7 6.7e6 8.13e6 3.22e6 1.04e6];

>> k=[1 4 10 1];

>> SD

***** End of Input, Start of Output of SD  ******
```

Iter'n	Func-count	f(x)	Norm of step	First-order optimality	CG-iterations
1	6	5.71298	1	12	0
2	11	0.671917	0.674657	21.4	2
3	16	0.44052	0.101216	584	1
4	21	0.437665	0.00949937	90.9	2
.	.	.	.	.	.
.	.	.	.	.	.
21	106	0.430799	0.0026304	26.6	2
22	111	0.430796	5.47022e-005	0.879	2
23	116	0.430796	0.00365723	0.879	2
24	121	0.430796	0.000914306	0.879	0
25	126	0.430796	0.000228577	1.38	0

Optimization terminated successfully:
Relative function value changing by less than OPTIONS.TolFun

SS = 0.65635

k = 0.75679 3.7305 8.958 0.63014

****** Below are the time, Ld, Lx and Ld - Lx *****
ans =

0	3.8854	3.8854	0
1	4.3802	4.5606	-0.18038
2	6.0294	5.8709	0.15849
3	7.2967	7.1935	0.10316
4	7.9814	8.1966	-0.21523
5	8.3139	8.313	0.00089015
6	8.0334	8.1032	-0.069814
7	8.2201	7.8485	0.3716
8	7.7316	7.5845	0.14707
9	7.0294	7.3176	-0.28822
10	6.8261	7.0495	-0.22341
11	6.9101	6.7808	0.12926
12	6.5079	6.5119	-0.0040548
14	6.017	5.9737	0.043297

***** End of output from SD.

After running SD, we usually run PredODE, which calculates μ, λ, and R_g and makes a smoother graph of the predicted U than SD does.

****** Input command to execute PredODE *******

>> PredODE

****** Output of PredODE

MuL =
1.3385

lL =
10

Lambda =
0.517

Rg =
4.3431

****** End of output from PredODE **********

References

Bailey, J.E., Ollis, D.F., 1986. Biochemical Engineering Fundamentals. McGraw-Hill, New York.

Baranyi, J., Roberts, T.A., 1994. A dynamic approach to predicting bacterial growth in food. Int. J. Food Microbiol. 23, 277–294.

Baranyi, J., Roberts, T.A., 1995. Mathematics of predictive food microbiology. Int. J. Food Microbiol. 25, 199–218.

Baranyi, J., Roberts, T.A., 2000. Principles and applications of predictive modeling of the effects of preservative factors on microorganisms. In: Lund, B.M., Baird-Parker, T.C., Gould, G.W. (Eds.), The Microbiological Safety and Quality of Food, vol. 1. Aspen Publishers, Gaithersburg, pp. 342–358.

Baranyi, J., Roberts, T.A., McClure, P.J., 1993. A non-autonomous differential equation to model bacterial growth. Food Microbiol. 10, 43–59.

Bassler, B.L., 1999. How bacteria talk to each other: regulation of gene expression by quorum sensing. Curr. Opin. Microbiol. 2 (6), 582–587.

Bray, H.G., White, K., 1966. Kinetics and Thermodynamics in Biochemistry. Academic Press, New York, pp. 364–404.

Del Nobile, M.A., D'Amato, D., Altieri, C., Corbo, M.R., Sinigaglia, M., 2003. Modeling the yeast growth-cycle in a model wine system. J. Food Sci. 68 (6), 2080–2085.

England, R.R., Hobbs, G., Bainton, N.J., Roberts, D.M., 1999. Microbial Signaling and Communication, 57th Symposium of the Society for General Microbiology. Cambridge University Press, Cambridge.

Epstein, I.R., Pojman, J.A., 1998. An Introduction to Nonlinear Chemical Dynamics. Oxford University Press, New York.

Feeherry, F.E., Doona, C.J., Taub, I.A., 2003. Effect of water activity on the growth kinetics of *Staphylococcus aureus* in ground bread crumb. J. Food Sci. 68 (3), 982–987.

Feeherry, F.E., Ross, E.W., Doona, C.J., 2004. A quasi-chemical model for the growth and death of microorganisms in foods by non-thermal and high pressure processing. Int. J. Food Microbiol. (in press).

Fussman, G.F., Ellner, S.P., Shertzer, K.W., Hairston, N.G., 2000. Crossing the Hopf bifurcation in a live predator–prey system. Science 290, 1358–1360.

Goldbeter, A., 1991. Biochemical Oscillations and Cellular Rhythms. Cambridge University Press, London.

Hinshelwood, C.N., 1953. Autosynthesis. J. Chem. Soc., 1947–1956.

Jones, J.E., Walker, S.J., 1993. Advances in modeling microbial growth. J. Ind. Microbiol. 12, 200–205.

Jones, J.E., Walker, S.J., Sutherland, J.P., Peck, M.W., Little, C.L., 1994. Mathematical modeling of the growth, survival, and death of *Yersinia enterocolitica*. Int. J. Food Microbiol. 23, 433–447.

Legan, D., Vandeven, M., Stewart, C., Cole, M., 2002. Modeling the growth, survival, and death of bacterial pathogens in foods. In: de W. Blackburn, C., McClure, P.J. (Eds.), Foodborne Pathogens: Hazards, Risk Analysis, and Control. Woodhead Publishing, Cambridge, pp. 53–95.

Leroy, F., De Vuyst, L., 2004. Growth of the bacteriocin-producing *Lactobacillus sakei* strain CTC 494 in MRS broth is strongly reduced due to nutrient exhaustion: a nutrient depletion model for the growth of lactic acid bacteria. Appl. Environ. Microbiol. 67 (10), 4407–4413.

Lynch, J.M., Poole, N.J., 1979. Microbial Ecology: A Conceptual Approach. John Wiley & Sons, New York.

McMeekin, T.A., Olley, J.N., Ross, T., Ratkowsky, D.A., 1993. Predictive Microbiology: Theory and Application. Research Studies Press, Somerset.

McMeekin, T.A., Brown, J., Krist, K., Miles, D., Neumeyer, K., Nichols, D.S., Olley, J., Presser, K., Ratkowsky, D.A., Ross, T., Salter, M., Soontranon, S., 1997. Quantitative Microbiology: a basis for food safety. Emerg. Infect. Dis. 3 (4), 541–549.

Membré, J.M., Thurette, J., Catteau, M., 1997. Modeling the growth, survival, and death of *Listeria monocytogenes*. J. Appl. Microbiol. 82, 345–350.

Membré, J.M., Kubaczka, M., Chéné, C., 1999. Combined effects of pH and sugar on growth rate of *Zygosaccharomyces rouxii*, a bakery product spoilage yeast. Appl. Environ. Microbiol. 65 (11), 4921–4925.

Novick, R.P., 1999. Regulation of pathogenicity in *Staphylococcus aureus* by a peptide-based density-sensing system. In: Dunny, G.M., Winans, S.C. (Eds.), Cell–Cell Signaling in Bacteria. ASM Press, Washington, DC, pp. 129–146.

Peleg, M., 1996. A model of microbial growth and decay in a closed habitat based on a combined Fermi's and the logistic equation. J. Sci. Food Agric. 71, 225–230.

Smith, J.L., Fratamico, P.M., Novak, J.S., 2004. Quorum sensing: a primer for food microbiologists—review. J. Food Prot. 67 (5), 1053–1070.

Taub, I.A., Feeherry, F.E., Ross, E.W., Kustin, K., Doona, C.J., 2003. A quasi-chemical kinetics model for the growth and death of *Staphylococcus aureus* in intermediate moisture bread. J. Food Sci. 68 (8), 2530–2537.

Van Impe, J.F., Versyck, K.J., Vereecken, K.M., Geeraerd, A.H., Dens, E.J., Bernaerts, K., 1999. Predictive microbiology of structured foods: development of a unifying modeling framework and application to microbial interactions and the selection of advanced model building blocks. In: Tuijtelaars, A.C.J., Samson, R.A., Rombouts, F.M., Notermans, S. (Eds.), Food Microbiology and Food Safety into the Next Millenium. Ponsen & Looyen, Wageningen, Netherlands, pp. 913–918.

Vereecken, K.M., Devlieghere, F., Bockstaele, A., Debevere, J., Van Impe, J.F., 2003. A model for lactic acid-induced inhibition of *Yersinia enterocolitica* in mono- and co-culture with *Lactobacillus sakei*. Food Microbiol. 20, 701–713.

Whiting, R.C., 1995. Microbial modeling in foods. Crit. Rev. Food Sci. Nutr. 35 (6), 467–494.

Whiting, R.C., Cygnarowicz-Provost, M.L., 1992. A quantitative model for bacterial growth and decline. Food Microbiol. 9, 269–277.